Article

Impacts of hydrodynamics and benthic communities on phytoplankton distributions in a large, dreissenid-colonized lake (Lake Simcoe, Ontario, Canada)

Astrid N. Schwalb[1*], Damien Bouffard[2**], Ted Ozersky[1***], Leon Boegman[2], Ralph E.H. Smith[1]

[1] *University of Waterloo, 200 University Ave W, Waterloo, N2L 3G1, ON, Canada*
[2] *Queen's University, 58 University Ave Kingston, K7L 3N6, ON, Canada*
** Corresponding author email: aschwalb@alumni.uoguelph.ca; current address: University of Lethbridge, 4401 University Drive, Lethbridge, T1K 3M4, AB, Canada*
*** Current address: Ecole Polytechnique Fédérale de Lausanne, 1015 Lausanne, Switzerland.*
**** Current address: Wellesley College, 106 Central St, Wellesley, MA, 02481, USA*

Received 5 February 2013; accepted 4 April 2013; published 30 April 2013

Abstract

We quantified the vertical and horizontal variation of chlorophyll *a* (Chl-*a*) to test how benthic filter feeders (dreissenid mussels), rooted macrophytes, and hydrodynamics influence phytoplankton distributions in a large lake (Lake Simcoe, Canada). Water column Chl-*a* did not differ significantly among sites of different depth, distance offshore, or rooted macrophyte biomass, but among the nearshore sites (7.5–10 m deep) it was higher where mussel biomass was greater. This counterintuitive result may be explained by wind-driven horizontal circulation during our specific study periods together with the patchy distribution of the mussels in the lake. Information on mixing depths, vertical eddy diffusivity, and mussel biomass was used to predict when and where the grazing pressure of mussels would likely deplete near-bottom phytoplankton. Chl-*a* depletion was frequently predicted at sites with moderate or high mussel biomass and sufficient thermal stratification to impede vertical mixing but never at sites without thermal stratification. Observations were consistent with predictions in most cases. The results suggested that mussels at depths of 7.5–15 m (a depth range of generally high mussel biomass in the lake) may frequently suffer food limitation due to near-bottom depletion during the early and middle stratified season. A deep Chl-*a* maximum was documented and may be important for mussel nutrition at such times.

Key words: benthic grazers, benthic-pelagic coupling, dreissenid mussels, hydrodynamics, phytoplankton

Introduction

Dreissenid mussels are successful aquatic invaders that spread rapidly throughout eastern North America following their arrival from Eurasia more than 20 years ago (Strayer 2009). The establishment of dreissenid mussels has drastically altered invaded aquatic ecosystems because of the ability of dreissenids to act as ecosystem engineers through the formation of mussel beds, biodeposition, and filtering activity (Karatayev et al. 2002, Vanderploeg et al. 2002). Among the most important effects of dreissenids are impacts on phytoplankton; dreissenids are able to significantly reduce phytoplankton biomass due to their high individual filtration rates and the high abundance they can reach (Kryger and Riisgård 1988, McMahon 1991, Higgins and Vander Zanden 2010).

The nearshore shunt hypothesis (Hecky et al. 2004) proposes that the impact of dreissenids on phytoplankton should be greater in the nearshore compared to the offshore, and that phytoplankton concentrations may be lower in the shallower and better mixed littoral areas compared to the offshore; however, the spatial distribution of mussel biomass and the prevailing hydrodynamics (e.g., thermal stratification and wind mixing) can modify

DOI: 10.5268/IW-3.2.596

the impacts of mussels on phytoplankton (Ackerman et al. 2001, Noonburg et al. 2003, Edwards et al. 2005, Boegman et al. 2008a, Zhang et al. 2008). During quiescent periods or in the presence of thermal stratification, the direct impact of dreissenids on phytoplankton in a lake can be weakened by the formation of a boundary layer above the bottom (Ackerman et al. 2001, Edwards et al. 2005, Boegman et al. 2008a). Under such conditions, mussels can cause near-bottom depletion of phytoplankton (e.g., Edwards et al. 2005) and suffer limitation of their feeding rates (Boegman et al. 2008a) while exerting less impact on phytoplankton in most of the water column. Mussel biomass, which influences maximum potential filtration rates, will help determine potential impacts on phytoplankton and the severity of hydrodynamic feeding limitation. Near-bottom reduction of phytoplankton has been detected above dense aggregations of dreissenids and marine mussels (Fréchette et al. 1989, Edwards et al. 2005, Nielsen and Maar 2007) but has not yet been studied in relation to spatial variations of dreissenid mussel biomass in lakes.

Considerable survey work between 2005 and 2009 (Jimenez et al. 2011, Ozersky et al. 2011; B. Ginn, Lake Simcoe Region Conservation Authority, unpubl. data; D. Evans, Ministry of Natural Resources, unpubl. data) provides an unusually detailed picture of mussel distributions for Lake Simcoe, Ontario, Canada (Fig. 1). Surveys have also shown that macrophyte biomass increased in Lake Simcoe following dreissenid establishment (Depew et al. 2011, Ginn 2011). Like the mussels, macrophytes have a heterogeneous distribution in Lake Simcoe (Ginn 2011). Macrophytes may influence phytoplankton biomass (Rooney and Kalff 2003) through a variety of mechanisms, including reduction of nutrient resuspension, allelopathic activity, and competition for nutrients (Mulderij et al. 2007). Few studies have attempted to link the spatial patterns of phytoplankton with those of dreissenid and macrophyte biomass in large lakes. The availability of recent and detailed survey data in Lake Simcoe presents a rare opportunity to investigate these links.

The objectives of this study were (1) to quantify the amount of vertical and horizontal variation in phytoplankton distribution in Lake Simcoe using chlorophyll *a* (Chl-*a*) fluorescence as a proximate measure for phytoplankton biomass; and (2) to identify potential drivers of variation in phytoplankton distribution with a focus on the effect of dreissenid mussels, macrophytes, and hydrodynamics. We predicted that: (1) near-bottom reduction of phytoplankton would occur in situations where mussel biomass was high and the turbulent mixing low, and we expected that (2) phytoplankton biomass would be generally lower nearshore compared to further offshore in accordance with the nearshore-shunt hypothesis (Hecky et al. 2004), but phytoplankton would also be decreased where mussel and macrophyte biomass was high.

Study site

Lake Simcoe is a large (722 km^2) dimictic hardwater lake, consisting of a main basin and 2 large bays (Palmer et al. 2011). Much of the main basin is shallow, and the mean depth of the lake is 14 m (Palmer et al. 2011). Zebra mussels (*Dreissena polymorpha*) arrived in Lake Simcoe in 1994 and were well established by 1996 (Evans et al. 2011). Quagga mussels (*D. rostriformis bugensis*) were first detected in the lake in 2004, but as of 2011 remained considerably less abundant than zebra mussels (T. Ozersky, Ontario Ministry of Natural Resources, October 2011, unpubl. data).

Methods

Sampling design

We sampled 3 types of sites: at-shore (AS) sites <5 m deep, near-shore (NS) sites 7.5–10 m deep, and near-offshore (NOS) sites 12.5–20 m deep, and used Chl-*a* fluorescence as a proximate measure for phytoplankton biomass.

Sampling sites were located mainly in the eastern part of the main basin in Lake Simcoe (Fig. 1). Mussels and macrophytes were surveyed with an underwater video system (Aqua-Vu Explorer 7, Nature Vision Inc., Brainerd, Minnesota, USA) to identify 3 AS sites with high biomass of macrophytes (>50 g m^{-2}) that were termed AS-MA stations (Table 1) and 4 stations (termed simply AS-stations) with moderate (11 g m^{-2}, station AS-1) to high biomass of dreissenid mussels (>20 g m^{-2} stations AS-2 to 4; Fig. 1, Table 1). The 3 stations with abundant macrophytes (AS-MA stations; Table 1) had negligible mussel biomass (≤1 g shell-free dry mass [SFDM] m^{-2}), and the 4 stations with abundant dreissenid mussels (AS-stations) had either no macrophytes or, in one case, low macrophyte biomass (10 g dry mass [DM] m^{-2}; Table 1).

Six nearshore sites were selected based on an existing map of mussel distribution (Fig. 1, based on data collected from 2005 to 2009) and video surveys conducted in 2011: 3 sites with higher dreissenid mussel biomass (>20 g m^{-2}, stations NS-1 to 3) and 3 with lower biomass (<20 g m^{-2}, stations NS-4 to 6; Fig. 1). In addition, 4 near-offshore sites were selected with negligible or no mussel biomass except for station NOS-2 that had high mussel biomass (Fig. 1). In total, we had 17 sites, 3 of which had high macrophyte biomass (only AS sites), 6 with lower mussel biomass or no mussels present

 DOI: 10.5268/IW-3.2.596

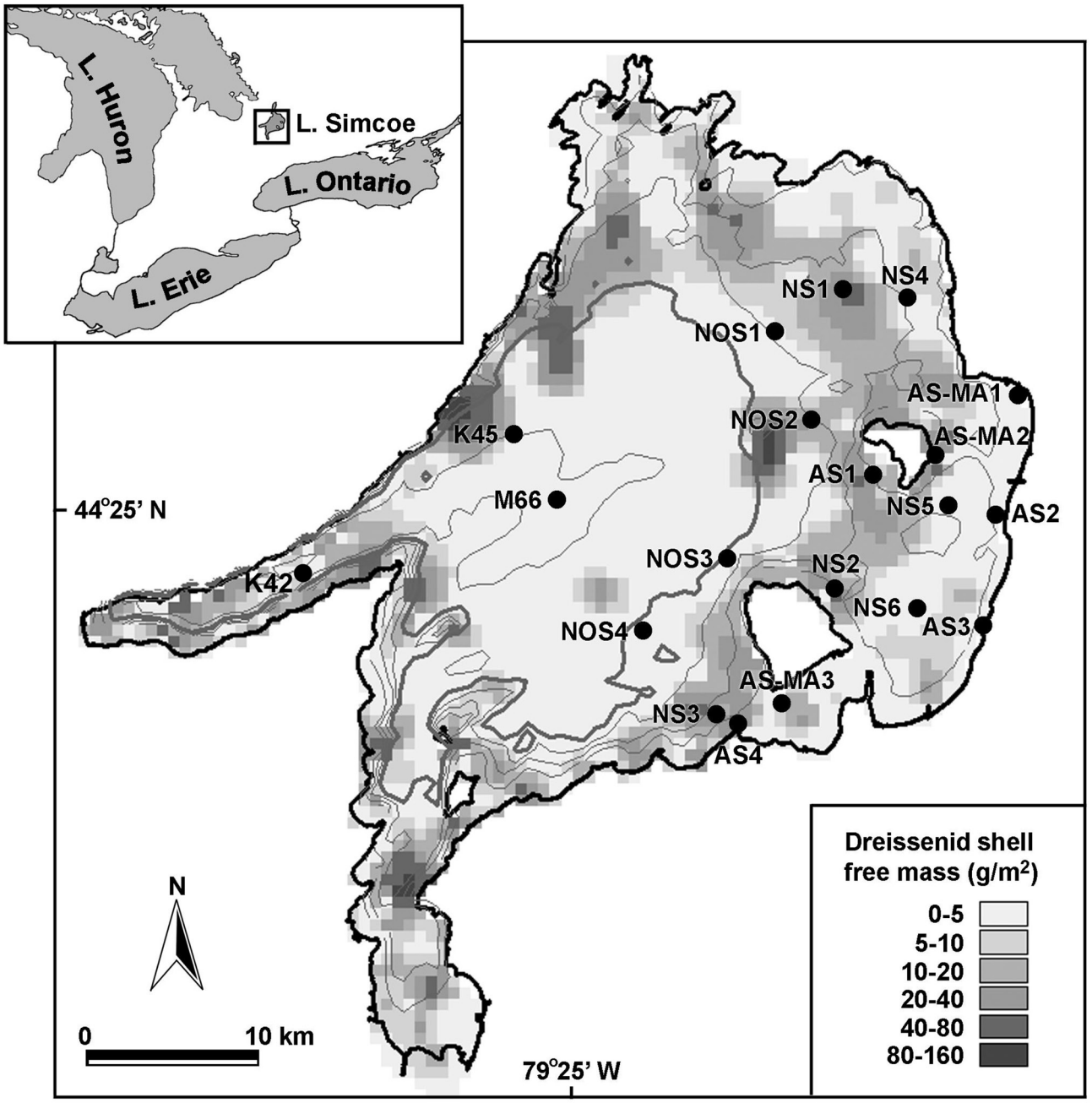

Fig. 1. Map of sampling stations and distribution of mussels in Lake Simcoe. NOS are near-offshore stations (12.5–20 m deep), NS are near-shore stations (7.5–10 m deep), AS are at-shore stations (<5 m deep), and AS-MA stations are at-shore stations with high macrophyte biomass. Stations K42, K45, and M66 are deeper offshore stations at which light profiles were measured.

(3 NS, 3 NOS), and 8 sites with higher mussel biomass (4 AS, 3 NS, 1 NOS).

Water column profiles of Chl-*a* fluorescence were taken with a FluoroProbe (calibrated with filtered water to account for the yellow substance level in the lake; TS 11-08, Moldaenke GmbH, Kiel, Germany), In *vivo* Chl-*a* measurements by fluorometer were highly correlated ($R^2 > 0.7$) with values measured on acetone extracts, and the relationship was not significantly different from 1:1, suggesting minimal bias from non-photochemical quenching or other interfering factors (Kim 2013). Profiles of temperature and dissolved oxygen (DO) were measured with a multiparameter water quality sonde (YSI-6600V2-4, YSI Inc, Yellow Spring, Ohio, USA; 4-6 measurements

Table 1. Depth of stations (rounded to closest meter), benthic biomass (mussels as shell free dry weight), sampling date for biomass, technique used for biomass estimation, and sampling dates for water column profiles in 2011. Video was used for rocky sites and ponar for soft-bottomed sites.

Station	Depth (m)	mussel/macrophyte biomass (g m^{-2})	Biomass sample collected	Technique used for biomass estimation	Water column profiles
AS-1	4	11/0	4 Oct	Video	28 Jul, 9 Sep
AS-2	3	35/0	4 Oct	Video	4 Aug, 9 Sep
AS-3	5	22/10	27 Jun	Ponar	28 Jul, 9 Sep
AS-4	3	32/0	27 Sep	Video	28 Jul, 9 Sep
AS-MA-1	3	0/70	07 Jul	Ponar	4 Aug, 9 Sep
AS-MA-2	3	1/54	07 Jul	Ponar	4 Aug, 9 Sep
AS-MA-3	3	0/145	27 Jun	Ponar	28 Jul, 9 Sep
NS-1	10	41/0	4 Oct	Video	4 Aug, 9 Sep
NS-2	8	30/0	29 Jul	Video	4 Aug, 9 Sep
NS-3	10	24/0	27 Jun	Video	28 Jul, 9 Sep
NS-4	9	15/0	4 Oct	Video	4 Aug, 9 Sep
NS-5	9	7/0	07 Jul	Ponar	4 Aug, 9 Sep
NS-6	9	3/0	27 Jun	Ponar	4 Aug, 9 Sep
NOS-1	13	1/0	7 Jul	Ponar	4 Aug, 9 Sep
NOS-2	14	78/0	27 Jun	Ponar	28 Jul, 9 Sep
NOS-3	20	0/0	29 Jul	Ponar	4 Aug, 9 Sep
NOS-4	20	0/0	9 Sep	Ponar	28 Jul, 9 Sep

per meter) twice at each station: once on 29 July or 4 August 2011 (hereafter termed "mid-summer"), and again on 9 September 2011 (hereafter termed "late summer"). Light profiles of the top 10 m of the water column were taken with a LI-COR Underwater Spherical Quantum Sensor (LI-189, LI-COR Biosciences, Lincoln, Nebraska, USA) on 12 August 2011 at stations K45 and M66 (Fig. 1) and on 12 September 2011 at stations K42 and M66 to characterize the photic depth (z_{eu}; 1% irradiance depth).

Benthic biomass and grazing rates

At sites with soft substrate, triplicate samples of mussels and macrophytes were obtained with a petite Ponar grab sampler (sampling area = 0.0231 m^2). Each site was sampled on one date between 27 June and 9 September 2011 (Table 1). Samples were washed over a 1 mm sieve to remove sediment, frozen, then dried at 60 ºC for 48 hours and weighed to determine DM. Mussel shells were removed to determine the SFDM. Macrophytes only occurred at sites with soft substrate, whereas mussels occurred at both softer and rocky substrate sites. At sites with rocky substrate, mussel biomass was estimated from video-based sampling conducted between 27 June and 4 October 2011 (Table 1). A number of replicate video quadrats were filmed at each site, and the mussel percent cover was estimated with quantitative, computerized analysis of 7 still frames of lake bottom at each site. Mussel percent cover was converted to mussel biomass using the empirical relationship described in Ozersky et al. (2011).

To estimate mussel grazing rates (α expressed as m^3 m^{-2} s^{-1}), individual clearance rates were calculated and then multiplied by the density of the mussels per site. The equation for individual clearance rates presented in Kryger and Riisgård (1988) was used: clearance rate = $6.82 \times (SFDM)^{0.88}$. Based on the range of SFDM for dreissenid mussels found in Lake Simcoe (0.6–23.5 mg $mussel^{-1}$; Ozersky et al. 2011), clearance rates ranged between 10 and 250 mL $mussel^{-1}$ $hour^{-1}$. The density of mussels for each site was estimated based on average determined biomass for each site (Table 1) and the average mass per mussel determined in Lake Simcoe (6.6 mg $mussel^{-1}$;

 DOI: 10.5268/IW-3.2.596

Ozersky et al. 2011). To capture the range of potential impact of very small to large mussels, minimum and maximum α were estimated for each site by multiplying the density of mussels per site with the minimum and maximum computed clearance rates.

Time scales

To test the prediction that near-bottom reduction of phytoplankton would occur in situations where mussel biomass was high and the turbulent mixing low, we quantified the potential impact of mussel biomass and turbulent mixing by estimating time scales for depletion of phytoplankton by grazing (T_G,) and for vertical turbulent diffusion (T_D) respectively (Koseff et al. 1993). Near-bottom reduction of phytoplankton biomass should occur when $T_G \leq T_D$, (i.e., grazing is strong [small T_G]) due to high local mussel biomass and vertical diffusivity because a measure for the turbulent mixing is weak (large T_D), whereas near-bottom reduction should not occur when $T_G > T_D$. Time scales for T_G and T_D were defined as

$$T_G = H/\alpha, \quad (1)$$

and

$$T_D = H^2/K_z, \quad (2)$$

where H (m) is the size of the well-mixed layer above the mussel bed, and K_z ($m^2\ s^{-1}$) is the vertical diffusivity. In the nonstratified case, H represents the entire water column, and 1 and 2 are similar to Koseff et al. (1993), Ackerman et al. (2001), and Boegman et al. (2008a). However, the presence of a thermocline, indicated by YSI profiles where temperature changed by >1 °C m^{-1} (Tables 2–3), restricts the impact of the mussels' filtration activity to the hypolimnetic water column. Vertical diffusivity in the thermocline was on average at least 5 times smaller than the K_z in the hypolimnion (see below) so we assumed that the flux through the thermocline was negligible and that H would represent the hypolimnion thickness only.

Hydrodynamics

The vertical diffusivity, K_z required in 2 to estimate T_D, was calculated differently for stratified and nonstratified stations. At non-stratified stations (Tables 2–3), the K_z was correlated to the wind intensity and estimated using the depth averaged turbulent diffusivity (Fischer et al. 1979, Loewen et al. 2007),

$$K_z = 0.067 \times H \times u^*, \quad (3)$$

where u* is the friction velocity depending on the wind speed (W):

$$u^* = \sqrt{\left(\frac{\rho_a}{\rho_w} \times C_{10} \times W^2\right)}, \quad (4)$$

with ρ_a and ρ_w the air and water density, respectively, and C_{10} the drag coefficient.

Under stratified conditions (Table 3), the vertical diffusivity is traditionally calculated as a function of the rate of dissipation, ε, and the buoyancy frequency, a measure for stratification,

$$N^2 = -\frac{g}{\rho} \times \frac{d\rho}{dz}, \quad (5)$$

where g is the gravitational acceleration, ρ is the fluid density, and z is the depth (Osborn 1980). The parameter ρ to calculate N^2 was estimated for each station using the temperature profiles measured with the YSI probe, see above). The rate of dissipation is difficult to measure and requires a microstructure profiler that was only used at some stations (see below). Instead, a simplified parameterization was used; this parameterization was initially described by Welander (1968) and Gargett and Holloway (1984) and depends only on the stratification:

$$K_z = a \times (N^2)^b, \quad (6)$$

where the parameters a and b account for the level of turbulence; b was found to vary from −0.41 (Heinz et al. 1990) to −1 (Gargett and Holloway 1984). For Lake Simcoe, a and b were calibrated (see details in Bouffard and Boegman 2013) with measurements from a microstructure profiler (SCAMP: Self Contained Autonomous Profiler, Precision Measurement Engineering Inc, Vista, California, USA) on 28 and 29 July 2011 at 8 stations: AS-1, AS-3, AS-4, AS-MA-3, NOS-4, NS-3, NOS-2, and NOS-4. Microstructures data (measurements of small fluctuations in temperature) allowed accurate estimate of ε and K_z and thus enabled field calibration of 6 to obtain a more accurate K_z parameterization (Bouffard and Boegman 2013). The fit of the coefficients a and b was done with our 26 collected microstructure profiles or 1664 vertical segments, and finally, we estimated the level of diffusivity for each stratified station using 6 and each nonstratified station using (3, Table 3).

To characterize the physical forcing conditions driving horizontal advection and vertical turbulent mixing, wind measurements from the Lake Simcoe buoy (Station 45151, 44°30′0″N; 79°22′12″W) operated by Environment Canada were obtained from the Fisheries and Oceans Canada website (DFO 2011) for the time period of 5 d prior to the actual sampling dates in August and September.

Table 2. Mid-summer (late July/early August) time-scales for grazing (T_G) and vertical diffusivity (T_D) at sites with non-zero mussel biomass. Predictions and observations are given for near-bottom Chl-*a* distributions. "Unresolved" observational outcomes occurred when the thermocline intersected the bottom. Unstrat indicates there was no stratification.

Station	Depth (m)*	Thermocline depth (m)	Grazing rate (min-max; $m^3\ m^{-2}\ d^{-1}$)	T_G (min-max; d)	T_D (d)	Prediction	Observational outcome
NS-1	9.8	9.1–9.3	1.4–37.3	0.02–0.4	>0.5	Reduction	Unresolved
NS-2	7.9	5.2–6.2	1.1–27.3	0.06–1.5	>4.2	Reduction	No sig. reduction ($R^2 < 0.01$, $p = 0.85$, $n = 22$)
NS-3	10.1	7.1–8.6	0.9–21.8	0.1–3.3	>13	Reduction	Sig. reduction ($R^2 = 0.84$, $p < 0.001$, $n = 15$; slope = –2.7)
NS-4	9.3	7.8–8.0	0.5–13.6	0.1–3.0	>3.2	Reduction	Sig. reduction ($R^2 = 0.70$, $p < 0.001$, $n = 16$; slope = –10.9)
NS-5	9.1	Unstrat.	0.2–6.4	1.4–45	~0.4	No reduction	No sig. reduction ($R^2 = 0.05$, $p = 0.16$, $n = 22$)
NS-6	9.1	Unstrat.	0.1–2.7	3.4–91	~0.4	No reduction	No sig. reduction ($R^2 = 0.10$, $p = 0.08$, $n = 25$)
NOS-1	13.3	10.4–11.5	0.2–5.4	0.3–9	>4.7	Reduction likely	Sig. reduction ($R^2 = 0.92$, $p < 0.001$, $n = 10$; slope = –7.4)
NOS-2	13.7	11.3–11.8	2.8–71	0.03–0.7	> 5.2	Reduction	Sig. reduction ($R^2 = 0.34$, $p < 0.01$, $n = 18$; slope = –0.9)
AS-1	4.4	Unstrat.	0.4–10	0.4–11	~0.2	No reduction	Sig. reduction ($R^2 = 0.46$, $p < 0.001$, $n = 20$; slope = –0.31)
AS-2	3.3	Unstrat.	1.3–31.9	0.1–2.5	~0.14	No reduction	Sig. increase ($R^2 = 0.62$, $p < 0.001$, $n = 24$; slope = +1.2)
AS-3	5.4	Unstrat.	0.8–20	0.27–6.7	~0.23	No reduction	Sig. reduction ($R^2 = 0.69$, $p < 0.001$, $n = 20$; slope = –1.7)
AS-4	3.2	Unstrat.	1.2–29.1	0.1–2.7	~0.14	No reduction	Sig. reduction ($R^2 = 0.71$, $p < 0.001$, $n = 3$; slope = –1.1)

*Note: station depths vary slightly between Tables 2 and 3 due to different navigation and water level variations with season.

Statistical analysis

To test whether dissipation decreased exponentially with depth we did a linear regression of depth versus log(dissipation). to quantify vertical variation and to test prediction from equation 1 that near-bottom reduction of phytoplankton would occur in situations where mussel biomass was high and the turbulent mixing low, we examined potential near-bottom phytoplankton depletion for each site with a linear regression of ln(Chl-*a*) versus ln(depth) of sampling points below the thermocline. A significantrelationship with a negative slope indicates a logarithmic decline of Chl-*a* with depth. In the absence of a thermocline, measurements of Chl-*a* from 0–2 m above the bottom (the depth that approximately corresponded to the hypolimnion when stratification was present) were used.

To examine horizontal variation in Chl-*a* concentrations, average Chl-*a* concentrations for the stations were first log-transformed to meet normality criteria. Average Chl-*a* concentrations for the entire water column did not differ significantly from those for the epilimnion (i.e., the well mixed surface layer above the thermocline, as judged from temperature profiles) when stratification existed (NS and NOS stations, paired *t*-test, $T_{19} = 0.5$, $p = 0.64$), so epilimnetic averages were used to compare Chl-*a* concentrations among stations. Paired *t*-tests were used to compare average epilimnetic Chl-*a* values for late July/early August with those from September to examine the effect of different sampling dates.

To test prediction (2), that phytoplankton biomass would be generally lower nearshore compared to further offshore, but phytoplankton would also be decreased where mussel and macrophyte biomass was high, differences in Chl-*a* among AS, NS-low and high mussel biomass, and NOS sites were analyzed with an analysis of variance (ANOVA) for the late summer samples and with a Kruskal-Wallis test for mid-summer

 DOI: 10.5268/IW-3.2.596

Table 3. Late summer (September) time-scales for grazing (T_G) and vertical diffusivity (T_D) at sites with non-zero mussel biomass. Predictions and observations are given for near-bottom Chl-*a* distributions. "Unresolved" observational outcomes occurred when the thermocline intersected the bottom. Unstrat indicates there was no stratification.

Station	Depth (m)	Thermocline depth (m)	Grazing rate (min-max; $m^3\ m^{-2}\ d^{-1}$)	T_G (min-max; d)	T_D (d)	Prediction	Observational outcome
NS-1	9.8	9.0–9.4	1.4–37.3	0.01–0.3	<0.5	Reduction	Unresolved
NS-2	7.5	Unstrat.	1.1–27.3	0.3–6.8	~0.3	No reduction	Sig. increase ($R^2 = 0.79$, $p < 0.001$, $n = 20$)
NS-3	10.1	Unstrat.	0.9–21.8	0.5–11.2	~0.4	No reduction	No sig. reduction ($R^2 = 0.13$, $p = 0.10$, $n = 15$)
NS-4	9.2	7.8–8.3	0.5–13.6	0.7–2	>1.2	No reduction	No sig. reduction ($R^2 = 0.01$, $p = 0.35$, $n = 7$)
NS-5	9.0	Unstrat.	0.2–6.4	1.4–45	~0.4	No reduction	Sig. increase ($R^2 = 0.59$, $p < 0.001$, $n = 17$)
NS-6	9.3	Unstrat.	0.1–2.7	3.4–93	~0.4	No reduction	No sig. reduction ($R^2 = 0.05$, $p = 0.16$, $n = 21$)
NOS-1	13.5	12.2–12.8	0.2–5.4	0.2–4.5	>0.7	No reduction	Unresolved
NOS-2	13.9	12.0–12.7	2.8–71	0.02–0.4	>2.5	Reduction	No sig. reduction ($R^2 = 0.08$, $p = 0.26$, $n = 8$)
AS-2	3.3	Unstrat.	1.3–31.9	0.1–2.5	~0.1	No reduction	Sig. increase ($R^2 = 0.72$, $p < 0.001$, $n = 18$; slope = +0.7)
AS-3	5.4	Unstrat.	0.8–20	0.3–6.7	~0.2	No reduction	Sig. increase ($R^2 = 0.72$, $p < 0.001$, $n = 18$; slope = +0.7)
AS-4	3.2	Unstrat.	1.2–29.1	0.4–10.7	~0.1	No reduction	Sig. increase ($R^2 = 0.33$, $p = 0.01$, $n = 15$; slope = +2.0)

because the criterion for homogeneity of variances was not met. Chl-*a* concentrations between AS mussel and macrophyte sites were not significantly different (see results), so AS sites were pooled prior to the ANOVA.

Results

Vertical diffusivity

The analysis of microstructure temperature data, which was used to estimate parameters needed to calculate K_z and ultimately T_D, showed that the rate of dissipation of turbulent kinetic energy decreased exponentially with station depth ($R^2 = 0.72$, $p = 0.002$, Fig. 2a) for mid-summer. This indicates that turbulence at shallower stations (especially AS sites) would be high (i.e., small T_D, see below). The best fit for K_z as a function of the background stratification, needed to estimate T_D for stratified stations, gave $a = 3.5 \times 10^{-7}$ and $b = -0.53$ for $N^2 < 10^{-4}\ s^{-2}$; and $a = 4.3 \times 10^{-10}$ and $b = -1.1$ for $N^2 > 10^{-4}\ s^{-2}$ (Fig. 2b). These values, with b ranging from approximately −1 to −0.5, are consistent with the literature (e.g., Imboden and Joller 1984) and the turbulence intensity parameterization, which has 2 different parameterizations depending on the buoyancy Reynolds number ($\varepsilon/\nu \times N^2$). K_z had a bi-modal distribution (Fig. 2c) with the lower peak at $\sim 5 \times 10^{-7}\ m^2\ s^{-1}$ in the thermocline region (high N^2) and a higher peak at $\sim 4 \times 10^{-5}\ m^2\ s^{-1}$ in the weakly stratified region including both the epilimnion and hypolimnion. The hypolimnion had an average diffusivity of $8 \times 10^{-6}\ m^2\ s^{-1}$ (not shown).

T_D was shorter at non-stratified versus stratified stations because of differences in wind induced mixing. At nonstratified stations, mixing depends directly on wind stress, with an average surface shear velocity u* of $\sim 5.5 \times 10^{-3}\ m\ s^{-1}$. In contrast, mixing at stratified stations depends on the wind induced bottom current, which is generated through baroclinic internal wave and up- and down-welling motions. As an example, at the nearshore station NS-3, SCAMP measurements indicated a rate of dissipation of $\varepsilon \sim 10^{-9}\ m^2\ s^{-3}$ at 1 m above the bottom. The resulting bottom shear velocity, assuming a logarithmic boundary layer, is $u^* = (\varepsilon / K_z)^{1/3} = 1.2 \times 10^{-3}\ m\ s^{-1}$, or 5 times lower than the surface shear velocity.

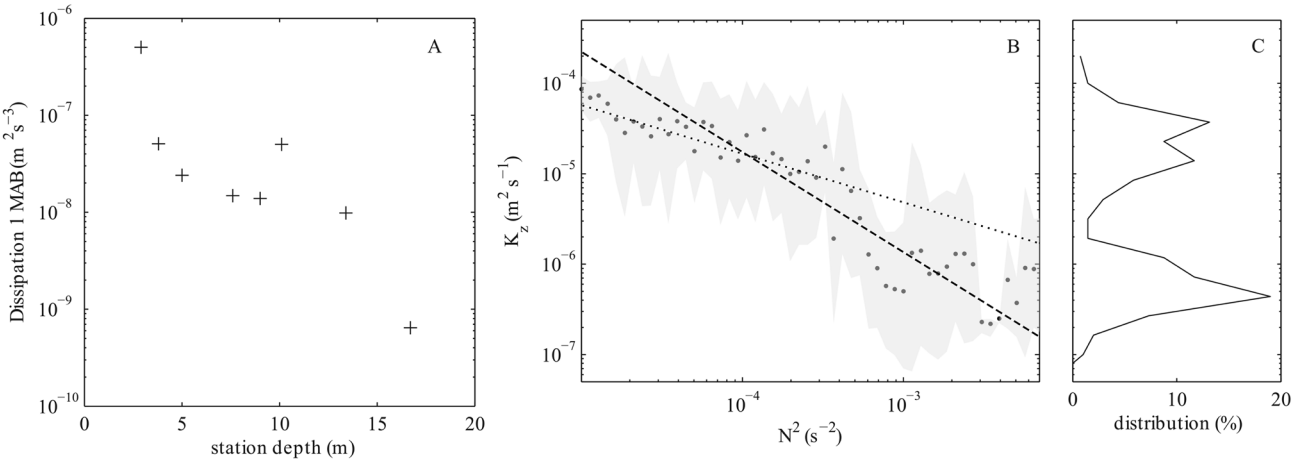

Fig. 2. Results for vertical diffusivity estimation. (A) Relationship between depth of the station and the dissipation measured on 28 and 29 July 2011. MAB stands for meters above the bottom. (B) Relationship between diffusivity (K_z) and buoyancy frequency (N^2); data have been averaged over similar N^2 (dots). and the 95% incertitude is shown by the shaded grey area. The dotted line represents the best fit for the weakly stratified case ($N^2 < 10^{-4}$ s^{-2}) and the dashed line for the strongly stratified case ($N^2 \geq 10^{-4}$ s^{-2}). (C) The frequency distribution of K_z across all observations.

Vertical distributions of Chl-*a*

Of the 14 cases in which we could both predict (based on T_G vs T_D) and test for near-bottom depletion of Chl-*a*, our predictions were confirmed in 12 cases (Tables 2 and 3). T_G was not a simple function of either mussel biomass or thermal stratification (Fig. 3); however, situations where T_G was clearly less than T_D occurred only with thermal stratification (Fig. 4). In mid-summer, T_G was less than T_D at all NS and NOS sites with moderate or high mussel biomass.

At AS-MA stations, T_G was extremely large or infinite and so no near-bottom depletion of phytoplankton was predicted (Tables 2 and 3). Measured profiles agreed with this prediction and even showed elevated Chl-*a* near bottom (Fig. 5). For AS-stations, T_G varied from slightly less than, to (usually) much more than, T_D (<0.25 days) in both mid-summer (Table 2) and late summer (Table 3), suggesting that near-bottom depletion should only occur with grazing near the upper end of the estimated range for these stations. Measured profiles did indicate decreases of Chl-*a* in mid-summer at 3 of the 4 AS stations (Fig. 5), although near-bottom increases were observed at the fourth station in mid-summer and, especially, late summer (Tables 2 and 3, Fig. 5, Fig. S1).

There were no macrophytes at any of the NS stations, and mussel biomass differed among the stations. Stations in areas where higher mussel biomass were expected based on mussel surveys in previous years (Fig. 1, Stations NS-1 to NS-3) had significantly higher mussel biomass (32 ± 5 g SFDM m^{-2}, n = 3) than those (Stations NS-4 to NS-6) in areas where lower biomass was expected (8 ± 4 g SFDM m^{-2}, n = 3, T_4 [subscript indicates the degrees of freedom] = 3.8, p = 0.02; Table 1). In mid-summer the minimum expected T_D was relatively low at ≤0.5 d at the unstratified stations NS-5 and NS-6 and at station NS-1, where the thermocline was weak and very close to the bottom (Table 2, Fig. 6). Minimum T_D was ≥3 d at the other NS stations, where a strong thermocline and larger hypolimnion thickness impeded mixing. The variations of

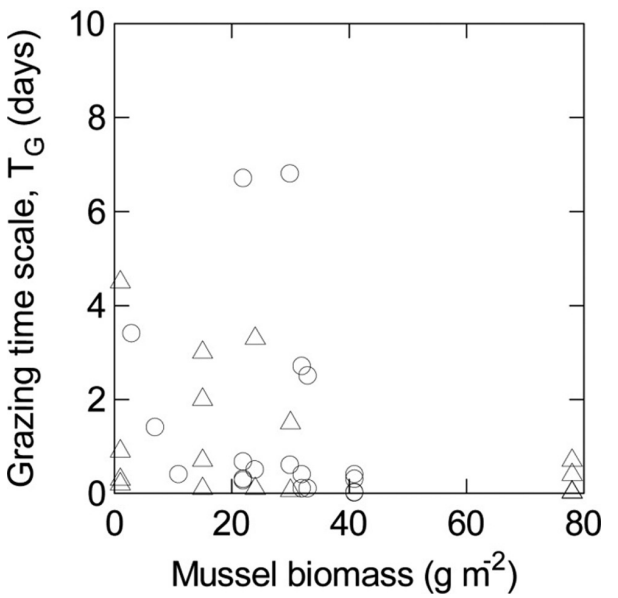

Fig. 3. Grazing time scales relative to mussel biomass for stratified (triangles) and unstratified (circles) sites. Two sites with $T_G > 30$ have been excluded to better visualize the majority of observations. For each site, the minimum and maximum T_G are plotted.

 DOI: 10.5268/IW-3.2.596

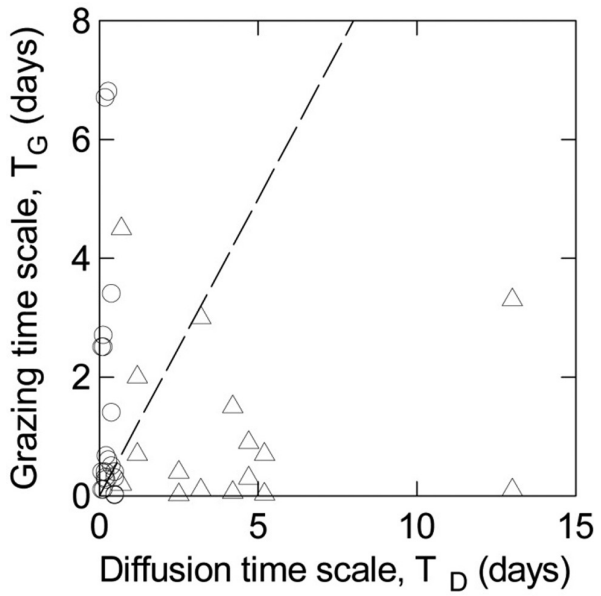

Fig. 4. Grazing time scales relative to diffusion time scales for stratified (triangles) and unstratified (circles) sites. Dashed line is 1:1, and the minimum and maximum T_G for each site are plotted. Points to the right of the 1:1 line represent situations in which near-bottom depletion of Chl-*a* is predicted to occur.

stratification and mussel biomass among NS sites led to predictions of near-bottom Chl-*a* depletion wherever mussel biomass was moderate or high (min $T_G < 0.1$), but not where it was low (min $T_G > 1.4$; Table 2). Not all predictions could be tested because the thermocline intersected the bottom at some sites, but where tests were possible the measured profiles usually agreed with predictions (Table 2, Fig. 6). In late summer, near-bottom depletion was neither predicted nor observed at most sites (Table 3, Fig. S2).

Among the deepest (NOS) stations, 2 (NOS-3 and NOS-4) had no detected mussel biomass (Table 1). No near bottom depletion was predicted and none was observed in either mid- or late summer (Fig. 7). The other NOS-stations were also thermally stratified in mid-summer (Fig. 7) and had large minimum T_D (>4.7 d; Table 2). In late summer the hypolimnion was smaller and minimum T_D decreased (>0.7 d; Table 3). Because of low turbulent mixing (high T_D) in mid-summer and high mussel biomass (only at NOS-2, low T_G) near-bottom Chl-*a* depletion was predicted (NOS-2) or seemed possible (NOS-1), and depletion was in fact observed at both sites in mid-summer (Table 2, Fig. 7) but not late summer (Table 3).

A deep chlorophyll maximum (DCM) was observed at NOS stations in mid-summer (Fig. 7), with a peak in the deeper part of the thermocline near 15 m. By comparison, the depth of the euphotic zone (1% light level) was 15–20 m. If the depth of the DCM was uniform among NOS stations then the bottom at the shallower NOS stations (NOS-1 and NOS-2) would have been in the upper portion of the feature, and there was a hint of it at NOS-2. Additional observations from deeper, offshore, stations (R.E.H. Smith, unpubl. data) suggest that a DCM with a peak at about 15 m is a common mid-summer feature in Lake Simcoe. An increase in DO of ~1–1.5 mg L^{-1} occurred at about the same depth as the mid-summer DCM (Fig. 7). In late summer, with a deeper thermocline, a clear DCM was not detected.

Horizontal distributions of Chl-*a*

In mid-summer epilimnetic Chl-*a* for NS and NOS stations (but not AS stations) was significantly lower compared to late summer (average difference: −0.8 ± 0.2 mg L^{-1}, paired *t*-test, $T_9 = 5.2$, $p < 0.001$; Fig. 8). In mid-summer, Chl-*a* concentrations were highest at AS stations and lowest at NS stations with low mussel biomass (Fig. 8) but differences among station categories were not significant (Kruskal-Wallis test, $H_3 = 3.7$, $p = 0.29$). However, Chl-*a* at NS stations with higher mussel biomass was significantly greater than at NS stations with lower mussel biomass when compared separately (*t*-test, $T_4 = 5.6$, $p < 0.01$). In late summer, the highest Chl-*a* concentrations were at NS stations with high mussel biomass and lowest at the AS stations, but differences were not statistically significant (ANOVA, $F_{3,13} = 2.2$, $p = 0.14$). NS stations with high mussel biomass also had greater Chl-*a* concentrations than NS stations with low mussel biomass in late summer, but the difference was not statistically significant (*t*-test, $T_4 = 1.2$, $p = 0.28$).

Within AS stations, variations in benthic community composition did not influence the observed Chl-*a*. Vertically-averaged Chl-*a* concentrations (surface to 0.5 m above bottom) were similar between AS (mussels but no macrophytes) and AS-MA (macrophytes but few mussels) sites with no significant difference in either mid-summer ($T_5 = 0.2$, $p = 0.85$) or late summer ($T_5 = 0.8$, $p = 0.44$) sampling periods.

Discussion

Our results suggest that mussels living at depths of 7.5–15 m in Lake Simcoe experience frequent depletion of food above the lake bottom during the summer stratified season. Near-bottom phytoplankton depletion has been found over marine mussel beds, but the biomass of mussels was several times to an order of magnitude higher (Fréchette et al. 1989, Dolmer 2000, Nielsen and Maar 2007) than in Lake Simcoe. Nonetheless, there is growing evidence that near-bottom phytoplankton depletion is an

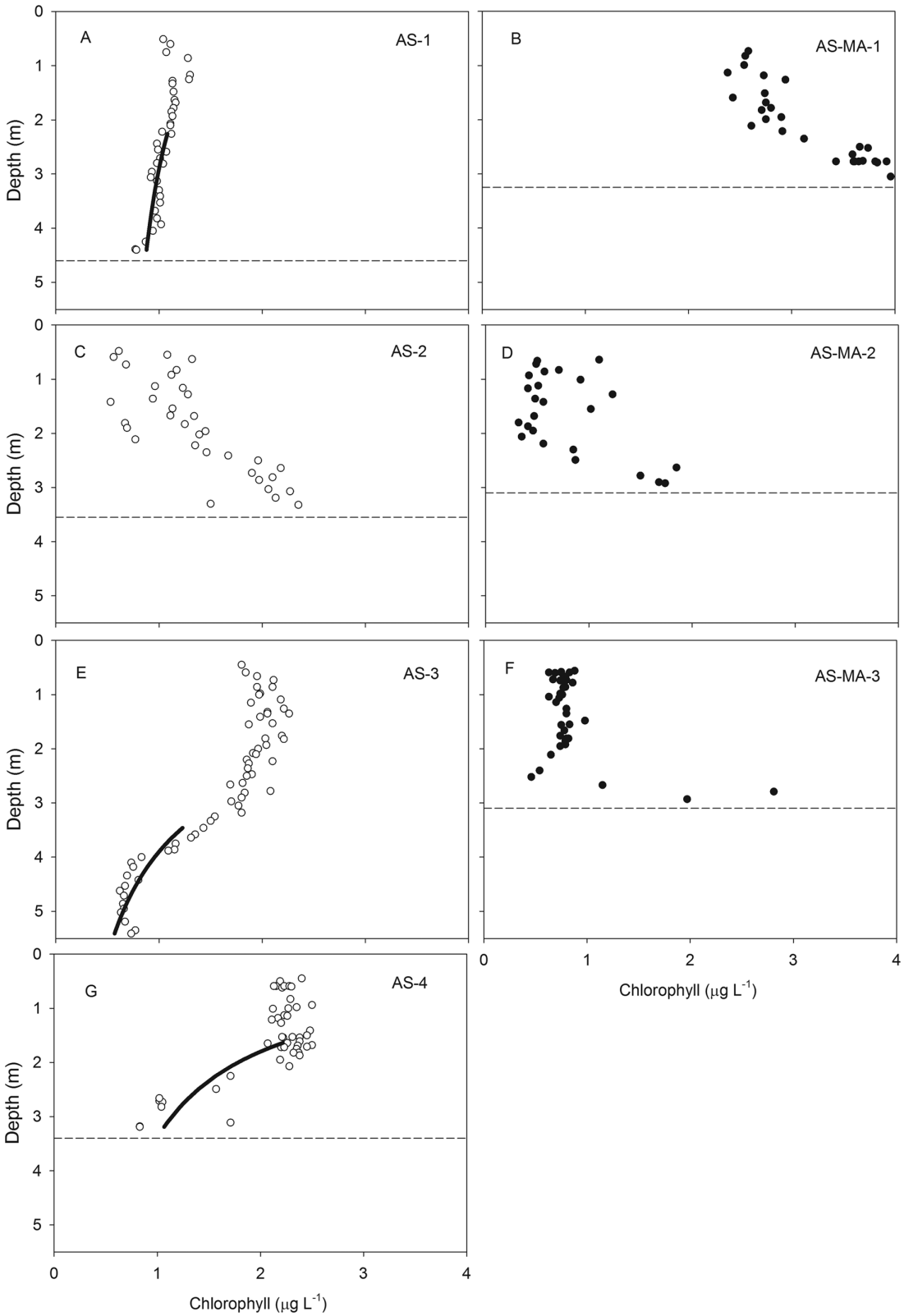

Fig. 5. Measured Chl-*a* concentrations in the water column for at-shore sites (<5 m deep) in mid-summer (July–Aug). Panels A, C, E, and G show sites with high dreissenid biomass while panels B, D, and F show sites with high macrophyte biomass. Dashed lines represent the lake bottom and solid lines represent significant ($P < 0.05$) negative regressions between ln(Chl-*a*) and ln(depth).

 DOI: 10.5268/IW-3.2.596

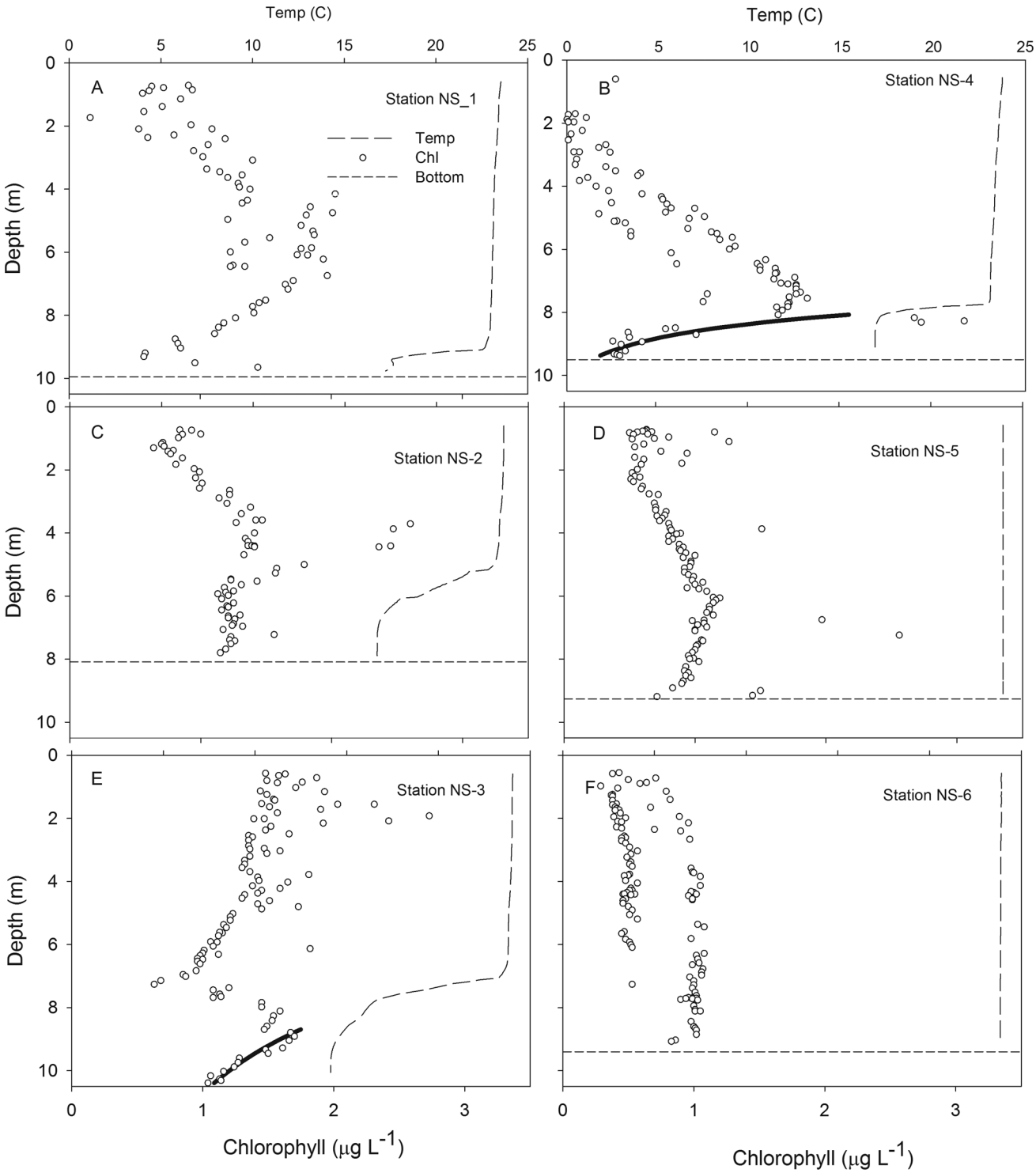

Fig. 6. Measured Chl-*a* concentrations in the water column at nearshore sites (7.5–10 m deep) for mid-summer (July–Aug). Panels A, C, E, and G show sites with high dreissenid biomass while panels B, D, and F show sites with high macrophyte biomass. Dashed lines represent the lake bottom and solid lines represent significant ($P < 0.05$) negative regressions between ln(Chl-*a*) and ln(depth).

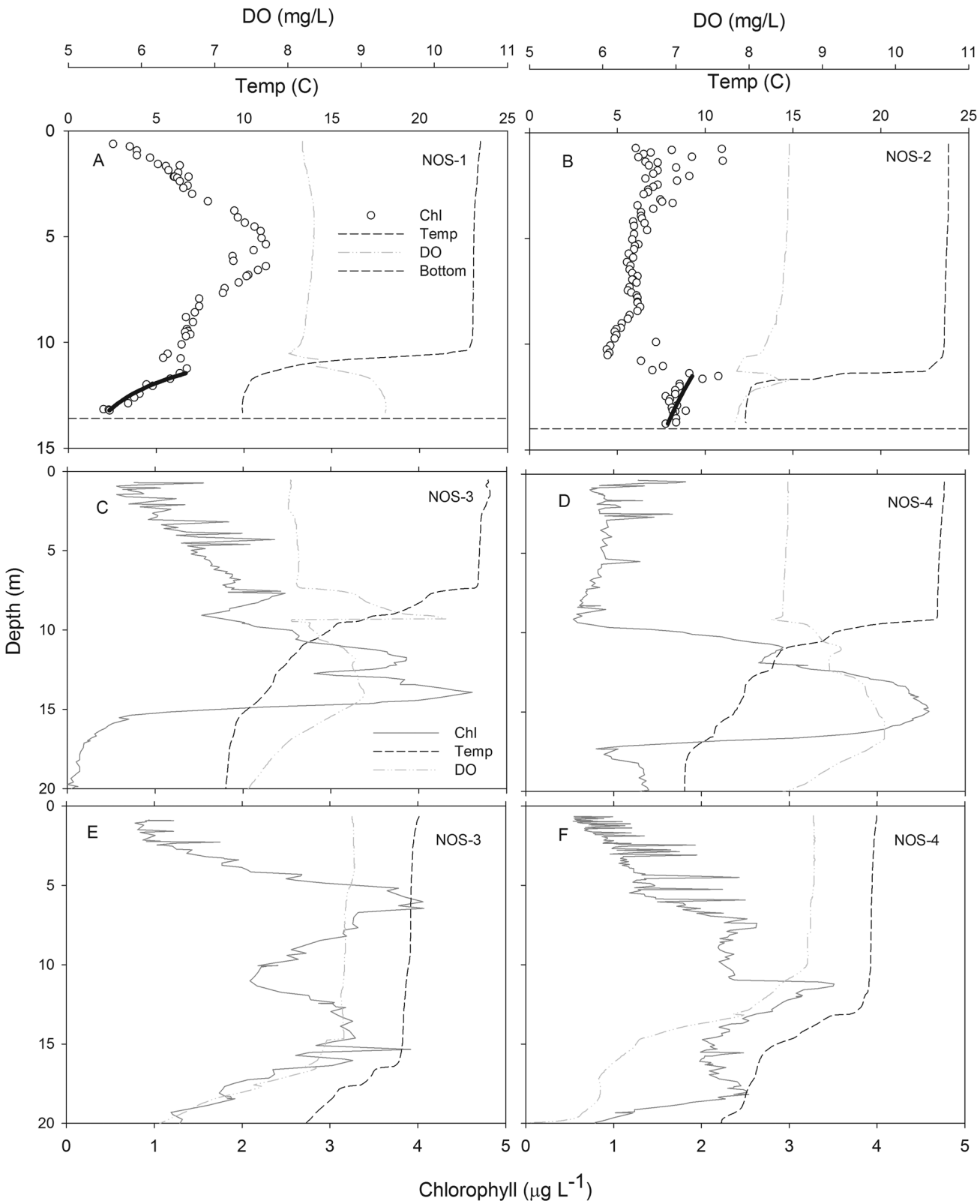

Fig. 7. Water column profiles for Chl-*a*, temperature, and DO at near-offshore sites (12.5–20 m deep) for (A–D) mid-summer and (E, F) late summer (stations NOS-1 and NOS-2 not shown). Dashed line at the bottom of panels A and B represents the lake bottom.

 DOI: 10.5268/IW-3.2.596

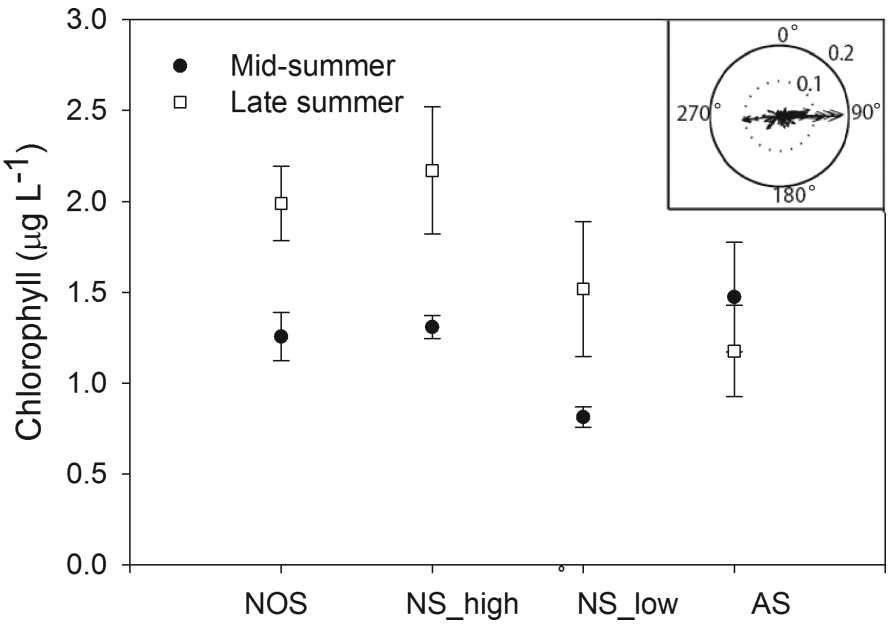

Fig. 8. Average Chl-*a* concentration (± 1 SE) in the epilimnion of near-offshore sites (NOS), near shore sites with high (NS_high) and low mussel biomasses (NS_low), and at-shore sites (AS) for mid-summer (late July/early Aug) and late summer (Sep). The inset shows the direction of the depth-averaged current at NS-2 for wind directions between 225 and 315º.

important limiting factor for dreissenid mussels in large lakes. Ackerman et al. (2001) documented near-bottom depletion of Chl-*a* and total organic seston over a mussel-colonized reef in western Lake Erie, at a depth of approximately 10 m. Although this depletion occurred in the absence of strong seasonal temperature stratification, the water column could be quite stable as a result of high solar input and light to moderate winds (<~6 m s^{-1}). Edwards et al. (2005) documented near-bottom phytoplankton depletion at even shallower (~5 m depth), but relatively sheltered, locations in western Lake Erie when winds were light. While our analysis indicated near-bottom depletion was largely limited to periods with a strong seasonal thermocline, it is likely that near-bottom depletion can also occur at shallower and unstratified sites when weather conditions are favourable. We saw evidence of this at some of our shallow (5 m) sites where mussel biomass was high.

Modelling of dreissenids in Lake Erie indicates that near-bottom depletion is an appreciable limit to their feeding. Predicted feeding rates were commonly half or less of those expected in the absence of the hydrodynamic limitation that results in creation of the near-bottom depletion zone (Boegman et al. 2008a), and mussel growth is likely affected as well. In Lake Ontario, mussels suspended 2 m off bottom, outside the near-bottom zone of depleted Chl-*a*, grew faster than those living on the bottom (Malkin et al. 2012), with bottom-dwelling mussels actually losing weight over the latter half of the summer. In Lake Simcoe, such hydrodynamic limitation (causing near-bottom depletion) could occur at a range of depths but seems especially likely for mussels in the 7.5–15 m depth interval, where high dreissenid biomass is commonly found and thermal stratification decreases turbulent mixing and thus facilitates near-bottom depletion.

The seasonal occurrence of a DCM may be important for alleviating early and mid-summer food limitation of mussels at intermediate depths in Lake Simcoe. Sufficient nutrients and light can support high levels of primary production and elevated biomass in DCMs (Fahnenstiel and Scavia 1987, Smith et al. 2005) and the DCMs observed in the current study were within the photic zone. However, elevated phytoplankton Chl-*a* content can also produce DCMs in the absence of biomass or production maxima (Barbiero and Tuchman 2001). Our data do not resolve whether the DCMs in Lake Simcoe were biomass or production maxima, but the peak in DO often observed at or near the DCM suggested that photosynthetic production was elevated. The DCM typically descends with the seasonal thermocline from early to late summer (Fahnenstiel and Scavia 1987, Malkin et al. 2012) and may have presented an elevated food supply for mussels at shallower depths earlier in the summer. Furthermore, internal wave activity in Lake Simcoe (Bouffard and Boegman 2012) has the potential to make DCM plankton

available to mussels living at depths considerably shallower than the average observed depth of the DCM. In Lake Ontario, the DCM seems to be important in permitting growth of mussels at intermediate depths (10–15 m) in early summer, whereas mussels at such depths achieve either no or even negative growth in late summer when the DCM has deepened and dissipated (Malkin et al. 2012). Additional study of DCM biomass and productivity as well as mussel feeding and growth in Lake Simcoe would be warranted to better understand how mussels succeed in maintaining population biomass in the face of hydrodynamic limitation, which is likely to be persistent when seasonal stratification is present.

Predictions for the occurrence of near bottom Chl-*a* depletion would be improved if better information about mussel filtering rates was available. They also overlook the countervailing effects of phytoplankton growth. Phytoplankton growth could be important at times, but estimates of *in situ* growth rates in comparable Great Lakes waters (0.2–0.6 d^{-1}; Fahnenstiel et al. 2000; GL Fahnenstiel, National Oceanic and Atmospheric Administration, summer 2011, pers. comm.) suggest that time scales for phytoplankton growth (1.7–5 days) would usually be too long to greatly alter the outcomes, especially at depths where light may limit phytoplankton growth rates. Resuspension phenomena, which could be important at times, also have not been examined here. Resuspension may explain why elevated Chl-*a* near bottom was commonly observed at our shallow sites. Our measurements did not discriminate the nature of the material comprising such features, which could derive at least in part from the detrital material and benthic algae that commonly accumulate in mussel-colonized habitats (Karatayev et al. 2002, Vanderploeg et al. 2002, Hecky et al. 2004).

The observed horizontal variations of Chl-*a* did not support our expectation that concentrations would be lower in well-mixed nearshore waters compared to deeper offshore waters, as predicted by the nearshore shunt hypothesis (Hecky et al. 2004). Chl-*a* in mid-summer at NS sites with higher mussel biomass (NS-1 to NS-3) was similar to the more offshore (NOS) sites. However, Chl-*a* concentration at NS sites with higher mussel biomass was significantly higher compared to NS sites with lower mussel biomass (NS-4 to NS-6) located closer to the western shore (Fig. 1), while AS sites (closest to shore) did not show a clear pattern (Fig. 8). We suggest that the ring of high mussel biomass at intermediate depths (Fig. 1) can present a "blockade" for offshore phytoplankton being transported toward the eastern shore, much as mussels in Lake Michigan are hypothesized to depress "downstream" plankton concentrations (Vanderploeg et al. 2010).

Wind and currents could also be driving the patterns we observed. During the mid-summer sampling, prevailing winds were west-southwest. The distribution of the depth-averaged current direction at station NS-2 estimated with a 3-D hydrodynamic model for west-southwest winds (Bouffard and Boegman 2012. Fig. 8) is similar at NS-1 and NS-3 (not shown) and indicate that the onshore advection is likely predominant under these forcing conditions.

A model for the joint influence of mussel grazing and horizontal advection supports the idea that the combined effect can explain the observed horizontal distributions. According to the calculations described in Appendix A, if phytoplankton is transported onshore by currents, it will be depleted by mussels over the 5–10 km distance, x, between nearshore sites with high mussel biomass (NS-1 to NS-3) and nearshore sites with low mussel biomass (NS-4 to NS-6). This occurs under a balance between horizontal advection and vertical turbulent diffusion (Fréchette et al. 1989, Butman et al. 1994). Depletion greater than 1 km < x < 10 km is strongly dependent on grazing, and qualitatively insensitive to variation in the range of current speeds typical for Lake Simcoe (see Appendix A and Fig. S3 for details).

Variations of horizontal current velocities across the region of interest could also influence differences among stations. The mean depth-averaged current is stronger at NS-2 than at NS-1 or NS-3 because of the topography contraction by the 2 islands (Fig. 1). Therefore, water that may have been depleted of Chl-*a* by mussel grazing would be replaced relatively quickly. This could explain why no near-bottom reduction of Chl-*a* was observed at NS-2 in early August, in contrast to our prediction.

Variations in wind direction and associated currents may also explain differences observed between sampling periods. The difference between NS sites with high and low mussel biomass was still present in September (Fig. 8), but the difference was not significant. Unlike the mid-summer sampling period, the late summer period had winds mainly from the south and east with a median wind direction of 144º 5 days prior to our sampling (i.e., SE-SSE). Offshore-to-nearshore advection would not be as strong as that observed in the earlier sampling period, so the proposed "filtering" effect of the outer stations with high mussel biomass would be less effective.

Our results show that several hydrodynamic effects, especially stratification and horizontal advection, can alter the impact of mussels on the distribution of phytoplankton, which may have several implications for other ecosystem processes. Hydrodynamic food limitation of mussels (e.g., Boegman et al. 2008b) can limit resources for benthic detritivores dependent on mussel deposits and would also limit rates of inorganic nutrient regeneration by mussels, depriving benthic algae of a potentially

 DOI: 10.5268/IW-3.2.596

important nutrient supplement (Ozersky et al. 2009) while lessening the beneficial (for benthic flora) effects of mussels on water transparency (Depew et al. 2011). Nevertheless, it should be advantageous for zooplankton because it lessens their direct competition with mussels. Horizontal advection as well as internal wave-mediated movements of deep Chl-*a* maxima can counteract local depletion of phytoplankton by mussels but are processes that vary strongly on a range of time scales and may not be captured well in typical field programs. All these considerations point toward a need for improved knowledge of hydrodynamic processes because they affect mussel energetics and associated ecosystem processes.

Acknowledgements

We thank Emilija Cvetanovska for her technical assistance in the field, Kamila Baranowska for providing LI-COR data for September 2011, Rebecca North for providing YSI-data, Luis Leon for producing the map, and 2 anonymous reviewers for helpful comments on an earlier version of this manuscript.

References

Ackerman JD, Loewen MR, Hamblin PF. 2001. Benthic–pelagic coupling over a zebra mussel reef in western Lake Erie. Limnol Oceanogr. 46:892–904.

Barbiero RP, Tuchman ML. 2001. Results from the U.S. EPA's biological open water surveillance program of the Laurentian Great Lakes: II. Deep chlorophyll maxima. J Great Lakes Res. 27:155–166.

Boegman L, Loewen MR, Hamblin PF, Culver DA. 2008a. Vertical mixing and weak stratification over zebra mussel colonies in western Lake Erie. Limnol Oceanogr. 53:1093–1110.

Boegman L, Loewen MR, Culver DA, Hamblin PF, Charlton MN. 2008b. Spatial-dynamic modelling of algal biomass in Lake Erie: relative impacts of dreissenid mussels and nutrient loads. J Environ Eng. 134:456–468.

Bouffard D, Boegman L. 2013. A diapycnal diffusivity model for stratified environmental flows. Dyn. Atmos. Oceans. http://dx.doi.org/10.1016/j.dynatmoce.2013.02.002

Bouffard D, Boegman L. 2012. Basin-scale internal waves. In: Bengtsson L, Herschy RW, Fairbridge RW, editors. Encyclopedia of lakes and reservoirs. New York (NY): Springer. p. 102–106.

Butman CA, Fréchette M, Geyer WR, Starczac VR. 1994. Flume experiments on food supply to the blue mussel *Mytilus edulis* L. as a function of boundary layer flow. Limnol Oceanogr. 39:1755–1768.

Depew DC, Houben AJ, Ozersky T, Hecky RE, Guildford SJ. 2011. Submerged aquatic vegetation in Cook's Bay, Lake Simcoe: Assessment of changes in response to increased water transparency. J Great Lakes Res. 37(suppl. 3):72–82.

[DFO] Department of Fisheries and Oceans [Internet]. 2011. Integrated Science Data Management Wave Data; [cited November 2011]. Available from: http://www.meds-sdmm.dfo-mpo.gc.ca/isdm-gdsi/waves-vagues/plot-trace/result-eng.asp?medsid=C45151&s1=1999-05&s2=2011-11.

Dolmer P. 2000. Feeding activity of mussels *Mytilus edulis* related to near-bed currents and phytoplankton biomass. J Sea Res. 44:221–231.

Edwards WJ, Rehmann CR, McDonald E, Culver DA. 2005. The impact of a benthic filter feeder: limitations imposed by physical transport of algae to the benthos. Can J Fish Aquat Sci. 62:205–214.

Evans DO, Skinner AJ, Allen R, McMurtry MJ. 2011. Invasion of zebra mussel, *Dreissena polymorpha*, in Lake Simcoe. J Great Lakes Res. 37(suppl. 3):36–45.

Fahnenstiel GL, Scavia D. 1987. Dynamics of Lake Michigan phytoplankton: the deep chlorophyll layer. J Great Lakes Res. 13:285–295.

Fahnenstiel GL, Stone RA, McCormick MJ, Schelske CL, Lohrenz SE. 2000. Spring isothermal mixing in the Great Lakes: evidence of nutrient limitation and nutrient-light interactions in a suboptimal light environment. Can J Fish Aquat Sci. 57:1901–1910.

Fischer HB, List EJ, Koh RCY, Imberger J, Brooks NH. 1979. Mixing in inland and coastal waters. San Diego (CA): Academic Press.

Fréchette M, Butman CA, Geyer WR. 1989. The importance of boundary-layer flows in supplying phytoplankton to the benthic suspension feeder, *Mytilus edulis* L. Limnol Oceanogr. 34:19–36.

Gargett AE, Holloway G. 1984. Dissipation and diffusion by internal wave breaking. J Mar Res. 42(1):15–27.

Ginn BK. 2011. Distribution and limnological drivers of submerged aquatic plant communities in Lake Simcoe (Ontario, Canada): Utility of macrophytes as bioindicators of lake trophic status. J Great Lakes Res. 37(suppl. 3):83–89.

Hecky RE, Smith REH, Barton DR, Guildford SJ, Taylor WD, Charlton MN, Howell T. 2004. The nearshore phosphorus shunt: a consequence of ecosystem engineering by dreissenids in the Laurentian Great Lakes. Can J Fish Aquat Sci. 61:1285–1293.

Heinz G, Ilmberger J, Schimmele M. 1990. Vertical mixing in Überlinger-See, western part of Lake Constance. Aquat Sci. 52(3):256–268.

Higgins SN, Vander Zanden MJ. 2010. What a difference a species makes: a meta–analysis of dreissenid mussel impacts on freshwater ecosystems. Ecol Monogr. 80:179–196.

Imboden DM, Joller TH. 1984. Turbulent mixing in the hypolimnion of Baldeggersee (Switzerland) traced by natural radon-222. Limnol Oceanogr. 29:831–844.

Jimenez A, Rennie MD, Sprules WG, La Rose J. 2011. Temporal changes in the benthic invertebrate community of Lake Simcoe, 1983–2008. J Great Lakes Res. 37(suppl. 3):103–112.

Karatayev AY, Burlakova LE, Padilla DK. 2002. Impacts of zebra mussels on aquatic communities and their role as ecosystem engineers. In: Leppäkoski E, Gollasch S, Olenin S, editors. Invasive aquatic species of Europe - Distribution, impacts and management. Dordrecht (The Netherlands): Kluwer Academic Publishers. p. 433–446.

Kim TY. 2013. Primary production by phytoplankton in Lake Simcoe,

2010-2011. [master's thesis]. [Waterloo (ON)]: University of Waterloo.

Koseff JR, Holen JK, Monismith SG, Cloern JE. 1993. Coupled effects of vertical mixing and benthic grazing on phytoplankton populations in shallow, turbid estuaries. J Marine Res. 51:843–868.

Kryger J, Riisgård HU. 1988. Filtration rate capacities in 6 species of European freshwater bivalves. Oecologia 77:34–38.

Loewen MR, Ackerman JD, Hamblin PF. 2007. Environmental implications of stratification and turbulent mixing in a shallow lake basin. Can J Fish Aquat Sci. 64:43–57.

Malkin SY, Silsbe GM, Smith REH, Howell TE. 2012. A deep chlorophyll maximum nourishes benthic filter feeders in the coastal zone of a large clear lake. Limnol Oceanogr. 57:735–748.

McMahon RF. 1991. Mollusca: Bivalvia. In: Thorp JH, Covich AP, editors. Ecology and classification of North American freshwater invertebrates. San Diego (CA): Academic Press. p. 315–399.

Mulderij G, Van Nes EH, Van Donk E. 2007. Macrophyte–phytoplankton interactions: The relative importance of allelopathy versus other factors. Ecol Model. 204:85–92.

Nielsen TG, Maar M. 2007. Effects of a blue mussel *Mytilus edulis* bed on vertical distribution and composition of the pelagic food web. Mar Ecol Prog Ser. 339:185–198.

Noonburg EG, Shuter BJ, Abrams PA. 2003. Indirect effects of zebra mussels (*Dreissena polymorpha*) on the planktonic food web. Can J Fish Aquat Sci. 60:1353–1368.

O'Riordan CA, Monismith SG, Koseff JR. 1995. The effect of bivalve excurrent jet dynamics on mass transfer in a benthic boundary layer. Limnol Oceanogr. 40:330–344.

Osborn, T. R. 1980. Estimates of local rate of vertical diffusion from dissipation measurements, J Phys Oceanogr. 10:83–89.

Ozersky T, Barton DR, Depew DC, Hecky RE, Guilford SJ. 2011. Effects of water movement on the distribution of invasive dreissenid mussels in Lake Simcoe, Ontario. J Great Lakes Res. 37(suppl. 3): 46–54.

Ozersky T, Malkin SY, Barton DR, Hecky RE. 2009. Dreissenid phosphorus excretion can sustain *C. glomerata* growth along a portion of Lake Ontario shoreline. J Great Lakes Res. 35:321–328.

Palmer ME, Winter JG, Young JD, Dillon PJ, Guilford SJ. 2011. Introduction and summary of research on Lake Simcoe: Research, monitoring, and restoration of a large lake and its watershed. J Great Lakes Res. 37(Suppl. 3):1–6.

Rooney N, Kalff J. 2003. Submerged macrophyte-bed effects on water-column phosphorus, chlorophyll a, and bacterial production. Ecosystems. 6:797–807.

Smith REH, Hiriart-Baer VP, Higgins SN, Guildford SJ, Charlton MN. 2005. Planktonic primary production in the offshore waters of dreissenid-infested Lake Erie in 1997. J Great Lakes Res. 31(Suppl. 2): 50–62.

Strayer DL. 2009. Twenty years of zebra mussels: lessons from the mollusk that made headlines. Front Ecol Environ. 7:135–141.

Vanderploeg HA, Liebig JR, Nalepa TF, Fahnenstiel GL, Pothoven SA. 2010. *Dreissena* and the disappearance of the spring phytoplankton bloom in Lake Michigan. J Great Lakes Res. 36:50–59.

Vanderploeg HA, Nalepa TF, Jude DJ, Mills EL, Holeck KT, Liebig JR, Grigorovich IA, Ojaveer H. 2002. Dispersal and emerging ecological impacts of Ponto-Caspian species in the Laurentian Great Lakes. Can J Fish Aquat Sci. 59:1209–1228.

Welander P. 1968. Theoretical forms for the vertical exchange coefficients in a stratified fluid with application to lakes and seas. Acta R Soc Sci Litt Gothob Geophys. 1:1–26.

Zhang H, Culver DA, Boegman L. 2008. A two-dimensional ecological model of Lake Erie: Application to estimate dreissenid impacts on large lake plankton populations. Ecol Model. 214:219–241.

 DOI: 10.5268/IW-3.2.596